

Electronic Supplementary Information

Electrocatalytic activity of silver decorated cerium dioxide toward oxygen reduction reaction and its application for high-performance aluminum-air battery

Shanshan Sun,^{a, c} Yejian Xue,^a Qin Wang,^{a, c} Shihua Li,^a Heran Huang,^a He Miao,^{b, *},

Zhaoping Liu^{a, *}

^a Key Laboratory of Graphene Technologies and Applications of Zhejiang Province and Advanced Li-ion Battery Engineering Lab, Ningbo Institute of Materials Technology and Engineering, Chinese Academy of Sciences, Zhejiang 315201, P.R. China.

^b Faculty of Maritime and Transportation, Ningbo University, Ningbo 315211, P.R. China.

^c University of Chinese Academy of Science, 19 A Yuquan Rd, Shijingshan District, Beijing, P.R. China 100049.

*Corresponding authors: Prof. Zhaoping Liu Tel.: +86-574-8668-6430

Fax: +86-574-8668-5096 E-mail: liuzp@nimte.ac.cn

*Corresponding authors: Dr. He Miao Tel.: +86-574-8668-5096

Fax: +86-574-8668-5096 E-mail: miaohe@nbu.edu.cn

The CeO₂ microspheres were prepared by a hydrothermal process, and the Ag-CeO₂ composites were fabricated according to the scheme as displayed in Fig.S1.

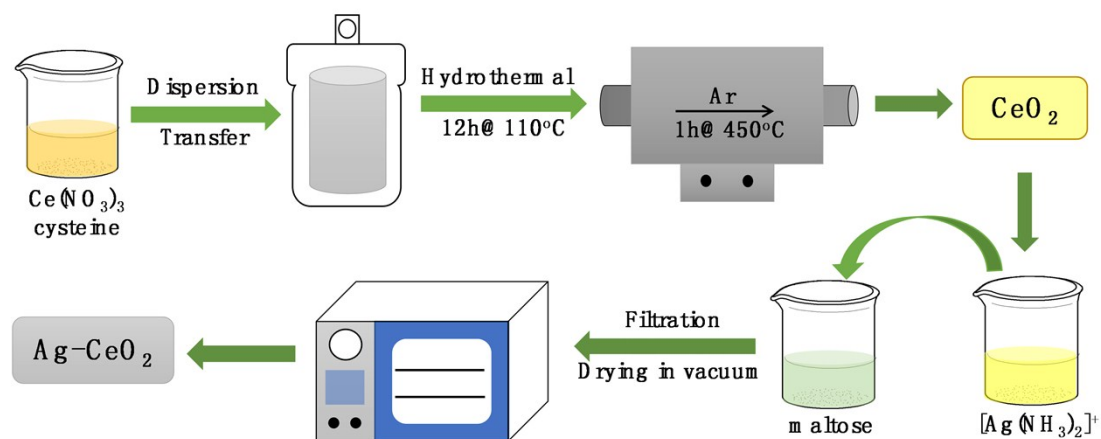


Fig. S1 Scheme of Ag-CeO₂ catalyst fabrication.

Ag and Ce contents were determined by inductively coupled plasma (ICP) atomic emission spectrophotometry (Perkin-Elmer, NexION 300) after dissolving the catalysts into a mixed solution of HCl and H₂O₂. According to ICP results, Ag-CeO₂ catalysts with different Ag contents were defined as 0.3% Ag-CeO₂, 1.5% Ag-CeO₂, 11.8% Ag-CeO₂, 19.4% Ag-CeO₂ and 47.6% Ag-CeO₂ all in weight ratio (Ag/CeO₂), respectively. The results are displayed in Table S1 as follows.

Table S1 Compositions of element Ag (wt.%) in Ag-CeO₂ complex obtained according to ICP and XPS results.

Sample	AgNO ₃ (g)	CeO ₂ (g)	ICP results (Ag%)	XPS results (Ag%)
CeO ₂	0	0.2	0	0
1# Ag-CeO ₂	0.016	0.2	0.3%	0.26%
2# Ag-CeO ₂	0.032	0.2	1.5%	0.38%
3# Ag-CeO ₂	0.064	0.2	11.8%	14.8%
4# Ag-CeO ₂	0.160	0.2	19.4%	18.3%
5# Ag-CeO ₂	0.240	0.2	47.6%	52.3%

The weight ratio of Ag in 1#~5# Ag-CeO₂ was increased with the addition of AgNO₃. It should be noted that the Ag content obtained from ICP results is a little different from that derived from XPS results. This difference could be caused by the different measurement mechanisms. The XPS is a common surface analytic method mainly used for chemical state determination with a depth of several micrometer. [1] The results of ICP which can determine the accurate content of element Ag were adopted because of the more accuracy than others.

The XRD patterns were collected on an AXS D8 Advance diffractometer by using Cu K α radiation ($\lambda = 0.15418$ nm). Fig.S2 shows the XRD patterns of CeO₂ and CeO₂ precursor.

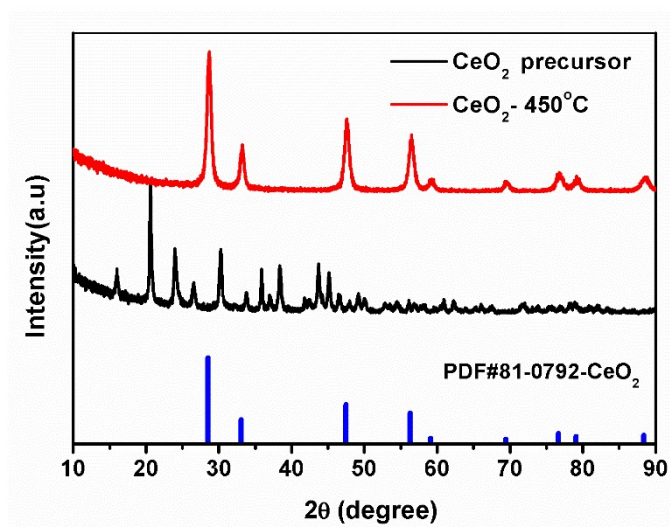


Fig. S2 XRD patterns of CeO₂ and CeO₂ precursor.

Fig.S3 is the XPS results of Ag 3d and Ce 3d performed on K-ratos AXISULTAR^{DLD} applying Al (mono) K α cathode source with the emission current of 8 mA and anode HT of 15 kV, respectively. The XPS spectra were calibrated with C 1s peak at 284.8 eV from the universal hydro-carbon contamination.

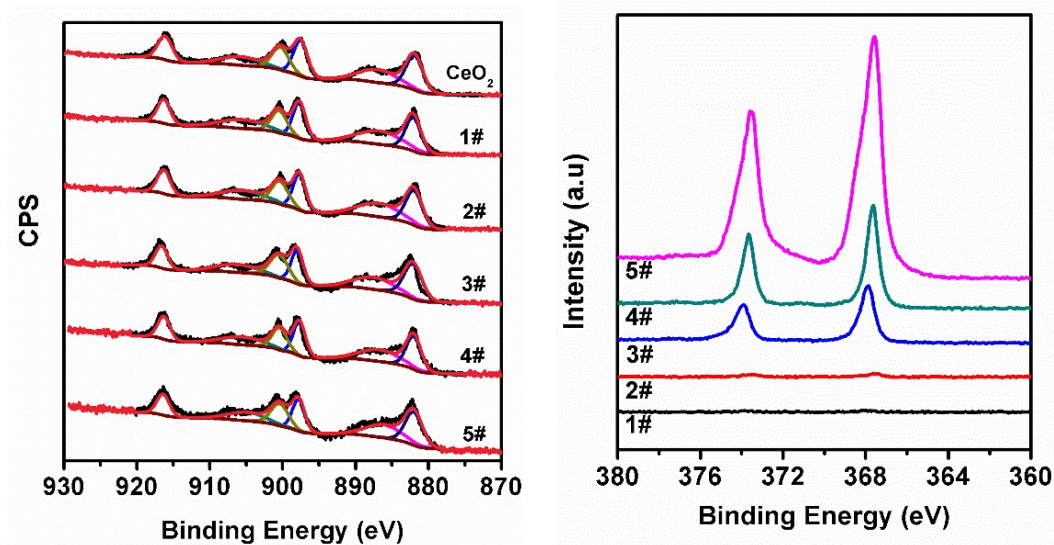


Fig. S3 XPS spectra of Ce 3d (a) and Ag 3d (b).

Fig.S4 displays the O_{1s} spectra of CeO₂ and 19.4% Ag-CeO₂. The spectra were fitted by two components located at *ca.* 529 eV and 531 eV, which correspond to lattice oxide oxygen and surface adsorbed oxygen-containing such as hydroxide or water. Note that the relative intensity and peak areas at 531 eV of 19.4% Ag-CeO₂ are higher than that of CeO₂, indicating the stronger oxygen affinity for 19.4% Ag-CeO₂ which facilitates the ORR process.

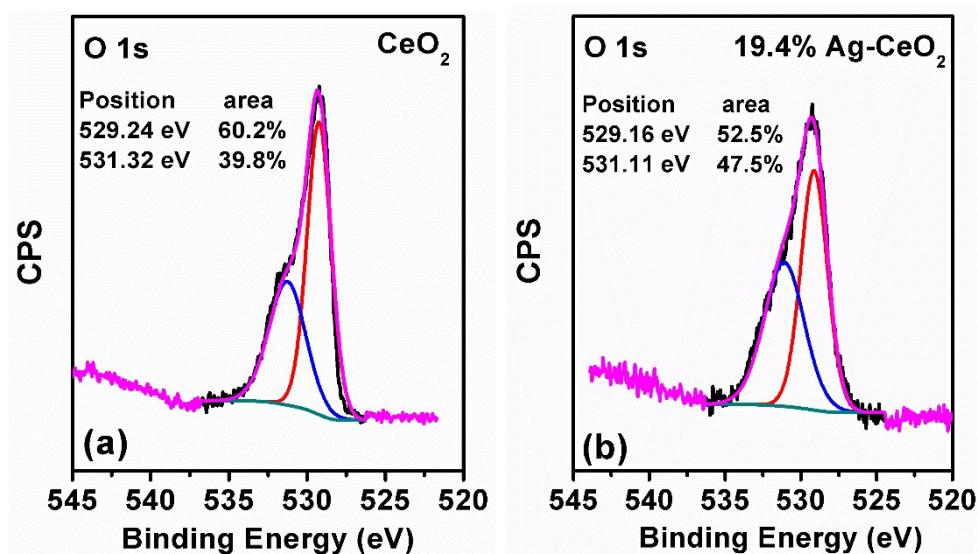


Fig. S4 O_{1s} XPS spectra of CeO₂ (a) and 19.4 Ag-CeO₂ (b).

The temperature-programmed desorption of oxygen analyses of the CeO₂, 19.4% Ag-CeO₂ and Ag were performed on Automatic 2920 (MICROMERITICS INSTRUMENT CORP, USA) under helium gas flow. The testing results are displayed in Fig.S5. In the typical TPD test, the sample ca. 0.08 g was loaded into the U-shape glass tube and evacuated for 1 h at 300°C. The sample was sequentially subjected to oxygen flow for 1h and evacuated for 1h at 600°C. Then the sample was cooled to 30°C in vacuum and exposed to oxygen flow again for adsorption. The heating rate was set at 10°C per minute. From Fig. S5, it can be noted that 19.4% Ag-CeO₂ displays the oxygen desorption peak at a much higher temperature at range of 100~300°C which indicates it has a stronger oxygen binding ability than Ag does.

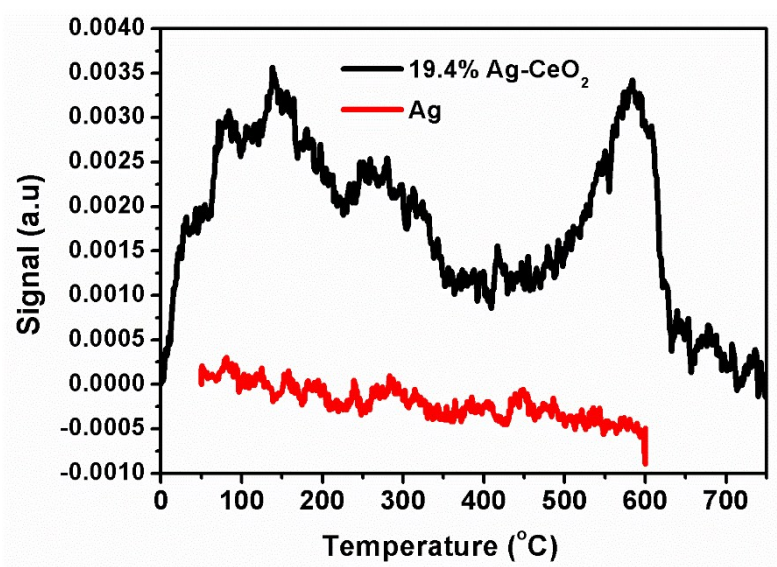


Fig.S5 O₂-TPD results of Ag and 19.4% Ag-CeO₂.

To confirm the particle size of Ag nanoparticles of 19.4% Ag-CeO₂, the high resolution TEM (HRTEM) images were recorded with a JEOL JEM-2100 microscope and the images are displayed in Fig.S6 as follows.

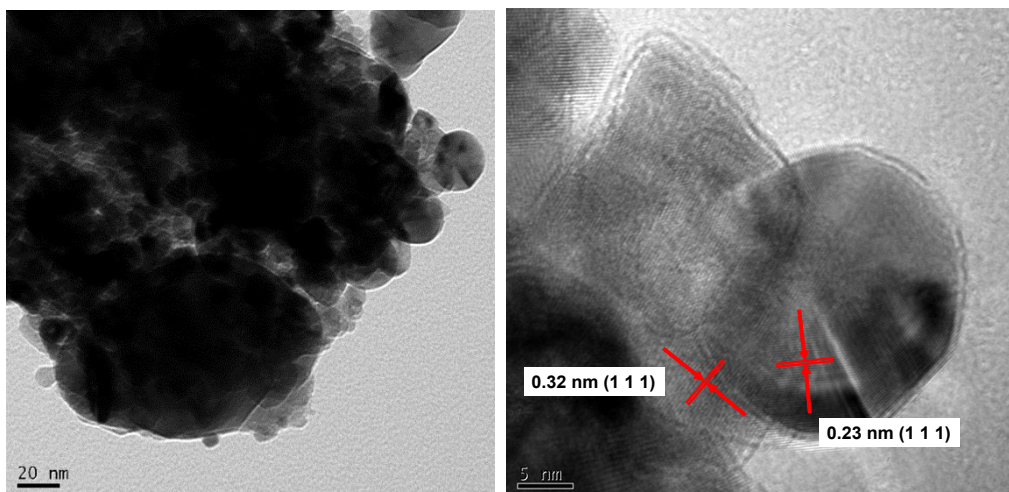


Fig. S6 TEM and HRTEM image of 19.4% Ag-CeO₂ catalyst.

Field emission scanning-electron microscope (SEM, Hitachi S-4800) was employed to examine the detailed morphologies and structures of the samples. The micro structures of Ag-CeO₂ (1#, 2#, 3# and 5#) with different Ag content are displayed in Fig.S7. When the loading of Ag is below 19%, the porous CeO₂ microspheres are not fully covered by Ag nanoparticles. When the content increased further, the excessive Ag nanoparticles without adhering on the porous CeO₂ appear.

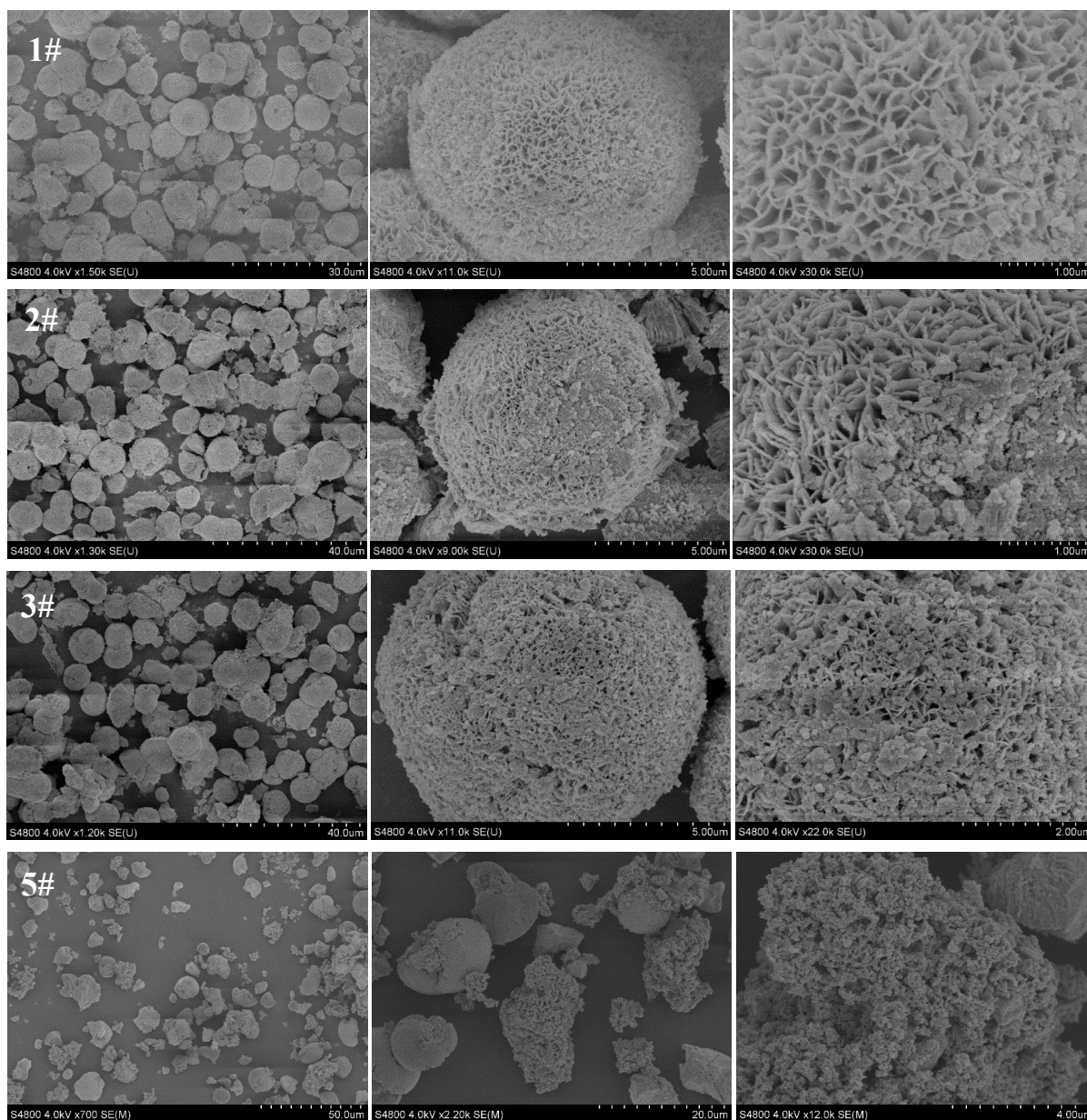


Fig. S7 SEM pictures of Ag-CeO₂ with different Ag contents (1#, 2#, 3# and 5#).

Rotating disc electrode (RDE) voltammetric was performed on a CHI1040B (Chenhua Corp.) workstation with a three-electrode system. The glassy carbon disk electrode with a diameter of 5 mm was used as the working electrode. Hg/HgO electrode was applied as the reference electrode and Pt wire was used as the counter electrode. The Hg/HgO electrode was calibrated with respect to the reversible hydrogen electrode (RHE) with the value of 0.923 V. Fig.S8 is the LSV curves of 19.4% Ag-CeO₂ with different catalysts loading from 0.12~0.75 mg cm⁻². The highest catalytic activity of Ag/CeO₂ is obtained with the catalyst loading of 0.50 mg cm⁻². The catalyst loading of 0.50 mg cm⁻² was prepared as follows. Firstly, 5 mg as-synthesized catalyst and 5 mg VXC-72 were distributed into 2 ml ethanol by 5 min ultrasonic dispersion. Then 90 μl 5wt% Nafion solutions (Dupont) was added into the above mixture with extra 25 min ultrasonic dispersion to form a well-dispersed ink. 20 μl of the ink was pipetted on the glassy carbon electrode and then evaporated to form a uniform and dry catalyst film. The linear sweeping voltammogram (LSV) was recorded at a rate of 5 mV s⁻¹ from 0.2 to -0.8 V (vs. Hg/HgO).

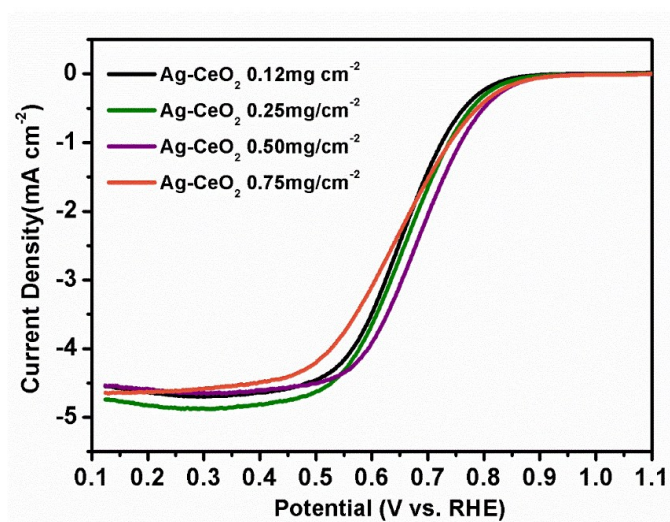


Fig. S8 LSV curves of 19.4% Ag-CeO₂ with different catalyst loadings.

The Koutecky-Levich (K-L) equations applied in this paper are as follows:

$$i^{-1} = i_L^{-1} + i_K^{-1} = (B\omega^{1/2})^{-1} + i_K^{-1} \quad (1)$$

$$B = 0.62nFC_0(D_0)^{2/3}\nu^{-1/6} \quad (2)$$

$$J_K = nFkC_0 \quad (3)$$

Where i is the measured current density, i_K and i_L are the kinetic and diffusion-limiting current densities, respectively, ω is the angular velocity of the disk, n is the overall number of electrons transferred in the oxygen reduction, F is the Faraday constant (96485 C mol⁻¹), C_0 is the concentration of O₂ (1.2×10⁻⁶ mol cm⁻³), ν is the kinematic viscosity of the electrolyte (0.01 cm² s⁻¹), and D_0 is the diffusion coefficient of O₂ in 0.1 M KOH (1.9×10⁻⁵ cm² s⁻¹).[2]

The LSV curves of Ag-CeO₂ samples from 1# to 5# with the catalyst loading of 0.50 mg cm⁻² on the glassy carbon electrode were also tested and displayed in Fig.S9. The 19.4% Ag-CeO₂ has the most positive curve which indicated the best ORR performance.

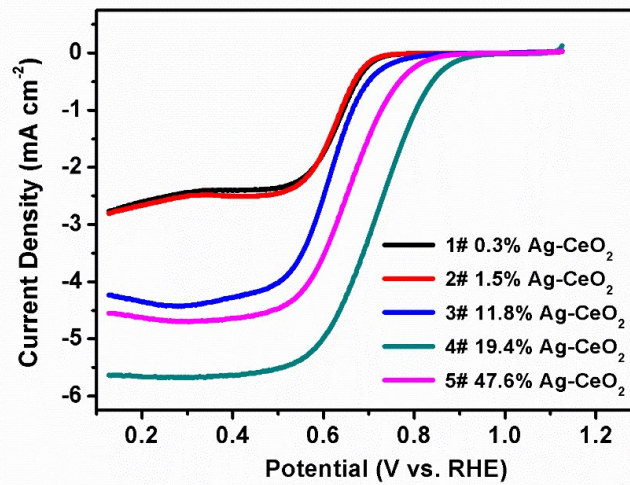


Fig. S9 LSV curves of Ag-CeO₂ with different Ag contents.

The RRDE testing was also performed to obtain more information about ORR happened on the as-prepared catalysts. The percentage of peroxides (HO_2^-) with respect to the total oxygen reduction products ($X_{\text{HO}_2^-}$) are calculated by the disk current (I_{disk}) the ring current (I_{ring}) and ring collection efficiency (N : 37%) with equation (4). The electron transferred number (n) is confirmed by equation (5). [3]

$$\chi_{\text{HO}_2^-} [\%] = 100 \frac{\frac{2I_{\text{ring}}}{N}}{I_{\text{disk}} + \frac{I_{\text{ring}}}{N}} \quad (4)$$

$$n = \frac{4NI_{\text{disk}}}{NI_{\text{disk}} + I_{\text{ring}}} \quad (5)$$

Fig.S10 (a) displays the I_{ring} and I_{disk} of catalysts collected by RRDE in O_2 -saturated 0.1 M KOH solution with the sweeping rate of 1600 rpm at room temperature. Fig.S10 (b) shows the curves calculated production of HO_2^- and electron transferred number (n).

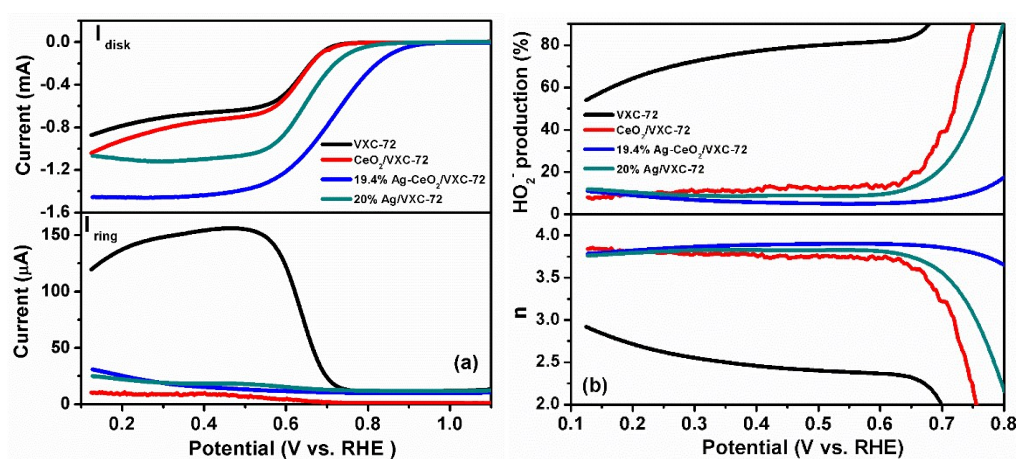


Fig. S10 RRDE experiments of VXC-72, CeO₂/VXC-72, 19.4% Ag-CeO₂ and 20% Ag/C in O_2 -saturated 0.1 M KOH solution with the sweeping rate of 1600rpm at room temperature.

In Fig3(d), the anodic peak of Ag-CeO₂/VXC-72 located at 1.146 V can be ascribed to the silver dissolution and the formation of a surface monolayer of Ag₂O

films. The anodic peaks located at 1.201 V and 1.280 V are caused by the formation of bulk phases of AgOH and Ag₂O, respectively. The cathodic peak at 1.05 V is ascribed to the electro-reduction of multi-layer Ag₂O.

The fabrication procedures of aluminum-air batteries were described as follows. [4] The air cathode of Al-air battery is a three-layer structure including catalytic layer, current collector and gas diffusion layer. The air cathode applying the as-prepared catalysts was fabricated by rolling catalyst paste and gas diffusion paste on the two sides of the current corrector. The catalyst paste was composed of as-prepared catalyst (0.18 g), active carbon (0.30 g) and acetylene black (0.15 g) dispersed by ethanol. The gas diffusion layer was the mixture of acetylene black and PTFE emulsion (60 wt.%) with a weight ratio of 2:3. The as-rolled air cathode was sintered in air at 350°C for 0.5 h and then the air cathode with active area of 2 cm×2 cm was tested in a homemade testing house. The electrolyte was 4 M KOH aqueous and the anode is multi-component (Al-Sn-Ga-Pb) Al anode. The diagrammatic structure of the home-made testing house was displayed in Fig.S11. I-V discharge curves were recorded by a multichannel battery testing system (CT2001A, Land Company) at room temperature. The long-term testing was conducted with renewing of Al anode about every 24 h and circulating of 4 M KOH electrolyte.

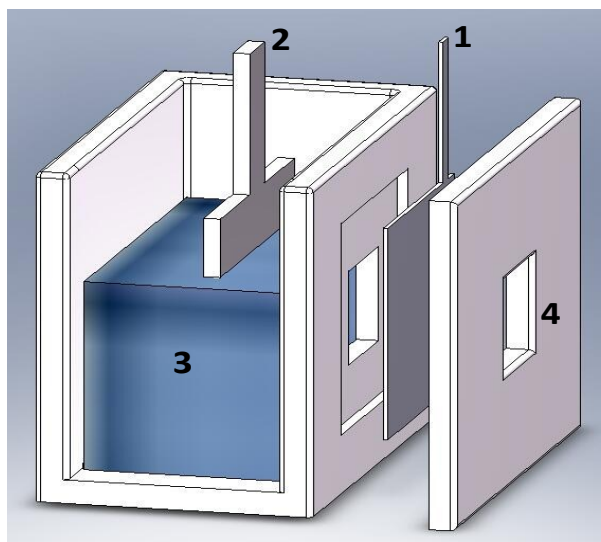


Fig. S11 Testing house used for aluminum-air battery measurements: 1-cathode, 2-Al alloy anode, 3-electrolyte (4 M KOH solution), 4-square area (2 cm×2 cm) opening to air.

Fig.S12 displayed the illustration of the Al-air battery with a LED lamp loaded. The catalyst used in the battery was 19.4% Ag-CeO₂. With the consumption of Al anode, the chemical energy was converted into the electrical energy. Obviously, with a better ORR catalyst, the conversion efficient would be much higher. The Al-air battery with Ag-CeO₂ catalyst exhibited high power density in the Al-air battery.

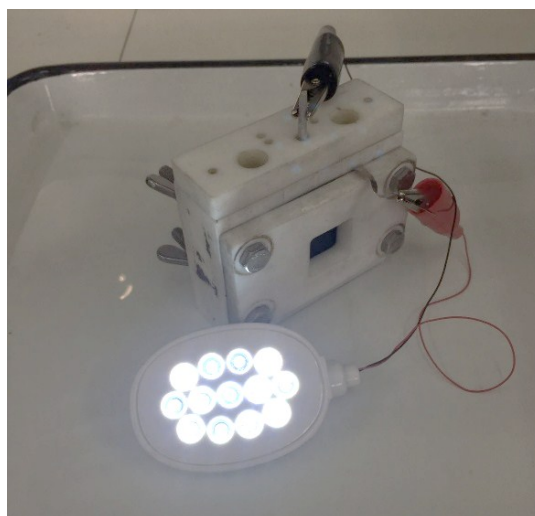


Fig. S12 Illustration of Al-air battery loaded with a LED lamp.

References

1. Fadley, C. S., *INSTRUMENTATION FOR SURFACE STUDIES – XPS ANGULAR-DISTRIBUTIONS*. Journal of Electron Spectroscopy and Related Phenomena, 1974. **5**(NOV-D): p. 725-754.
2. Davis, R.E., G.L. Horvath, and C.W. Tobias, *SOLUBILITY AND DIFFUSION COEFFICIENT OF OXYGEN IN POTASSIUM HYDROXIDE SOLUTIONS*. Electrochimica Acta, 1967. **12**(3): p. 287-290.
3. Paulus, U.A., et al., *Oxygen reduction on a high-surface area Pt/Vulcan carbon catalyst: a thin-film rotating ring-disk electrode study*. Journal of Electroanalytical Chemistry, 2001. **495**(2): p. 134-145.
4. Sun, S., et al., *Oxygen reduction reaction catalysts of manganese oxide decorated by silver nanoparticles for aluminum-air batteries*. Electrochimica Acta, 2016. **214**: p. 49-55.